NRL Memorandum Report 4295

An Analysis of Vibration Sensitivity in Hydrophone Design

GEORGE DICKSON HUGUS III

Transducer Branch
Underwater Sound Reference Detachment
PO Box 8337
Orlando, FL 32856

November 28, 1980

NAVAL RESEARCH LABORATORY
Washington, D.C.

SECURITY CLASSIFICATION OF THIS PAGE (When Data Entered)

REPORT DOCUMENTATION PAGE

READ INSTRUCTIONS BEFORE COMPLETING FORM

1. REPORT NUMBER: NRL Memorandum Report 4295	2. GOVT ACCESSION NO.: AD-A092 809
3. RECIPIENT'S CATALOG NUMBER:	
4. TITLE (and Subtitle): AN ANALYSIS OF VIBRATION SENSITIVITY IN HYDROPHONE DESIGN	5. TYPE OF REPORT & PERIOD COVERED: Final report on terminated NRL Problem
	6. PERFORMING ORG. REPORT NUMBER:
7. AUTHOR(s): George Dickson Hugus, III	8. CONTRACT OR GRANT NUMBER(s):
9. PERFORMING ORGANIZATION NAME AND ADDRESS: Underwater Sound Reference Detachment, Naval Research Laboratory, PO Box 8337, Orlando, FL 32856	10. PROGRAM ELEMENT, PROJECT, TASK AREA & WORK UNIT NUMBERS: 62711N-11; ZF11-121-003; 59-S099-0-1
11. CONTROLLING OFFICE NAME AND ADDRESS: Office of Naval Research, Arlington, VA 22217	12. REPORT DATE: November 28, 1980
	13. NUMBER OF PAGES: 18
14. MONITORING AGENCY NAME & ADDRESS (if different from Controlling Office): NRL-MR-4295	15. SECURITY CLASS. (of this report): UNCLASSIFIED
	15a. DECLASSIFICATION/DOWNGRADING SCHEDULE:

16. DISTRIBUTION STATEMENT (of this Report)

Approved for public release; unlimited distribution.

17. DISTRIBUTION STATEMENT (of the abstract entered in Block 20, if different from Report)

18. SUPPLEMENTARY NOTES

This report is taken from Mr. Hugus' thesis for a Masters Degree.

19. KEY WORDS (Continue on reverse side if necessary and identify by block number)

20. ABSTRACT (Continue on reverse side if necessary and identify by block number)

Hydrophones used in the ocean produce spurious outputs because of vibration sensitivity that can severely degrade measurement accuracy. Sources of these vibration inputs are ocean surface waves, flow turbulance, and induced non-acoustic mechanical vibration. The hydrophone response to these vibrations is a noise voltage output. This can lead to a signal-to-noise problem, particularly when measurements of small sound pressure levels are to be made. This report presents an analysis of the vibration responses of three typical

(Continues)

DD FORM 1 JAN 73 1473 EDITION OF 1 NOV 65 IS OBSOLETE S/N 0102-LF-014-6601

SECURITY CLASSIFICATION OF THIS PAGE (When Data Entered)

20. Abstract (Continued)

piezoelectric hydrophone sensor elements configurations and gives design methods and constraints for reducing the problem of vibration sensitivity to an acceptable level. The sensor element configurations analyzed are the radially polarized cylindrical shell, the radially polarized spherical shell, and the axially polarized cylindrical shell. The analysis is carried out for two effects. First an electromechanical analyses is given of the voltage sensitivity of each of the three sensor configurations to the inertial effect of acceleration inputs. The second effect analyzed is the voltage sensitivity of a pressure sensitive sensor element to the hydrostatic pressure amplitude caused by periodic vertical displacements of a hydrophone. Results of the first analyses show that the radially polarized cylindrical and spherical shell configurations and axially polarized cylindrical shell configuration have zero acceleration sensitivity to inputs on the axes of symmetry. The analyses of the second effect, hydrophone sensor response to periodic vertical displacements, show high voltage sensitivity to very small displacement amplitudes. Data are given for the maximum permissible vertical displacement amplitude to produce a 20-dB signal-to-noise ratio. Based on these analyses, design considerations are given to minimize hydrophone vibration sensitivity.

CONTENTS

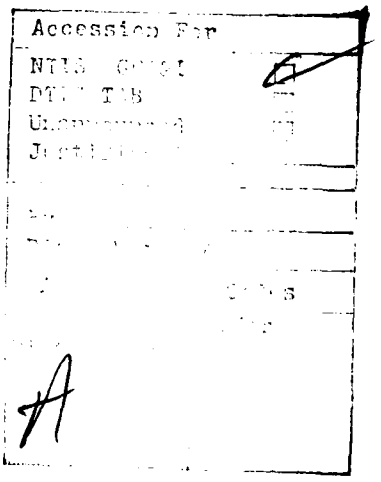

AN ANALYSIS OF VIBRATION SENSITIVITY IN HYDROPHONE DESIGN

INTRODUCTION

Hydrophones are often used at sea to calibrate other transducers and to make acoustic noise measurements. These need to be reference standards with an acoustic sensitivity constant with time, frequency, temperature, and depth. Despite this stability, spurious outputs occur that severely degrade measurement accuracy. Sources of these unwanted outputs are electrical self-noise and that due to external inputs, such as hydrodynamic flow turbulence and induced vibration.

Vibration is often an inherent condition in the use of hydrophones at sea. When suspended from a ship or buoy, a hydrophone can experience large vertical periodic displacements due to surface waves, subsurface waves, or subsurface currents. Vibration can be induced due to flow turbulence and vortex shedding of electrical and support cables. The hydrophone response to these vibrations becomes a noise voltage output. A requirement for acoustic measurements at sea is the ability to detect and measure very low sound pressure levels (SPL) [1,2]. These measurement conditions lead, therefore, to a low signal-to-noise ratio problem when the acoustic and vibration input frequencies are coincident. Also, due to vibration, the hydrophone sensor output voltage can exceed the dynamic range of the integral preamplifier causing electrical blockage and damage of the electronically unprotected input stage.

The purpose of this report is, therefore, to present the analyses of the response to vibration of typical hydrophone sensor configurations and to give design methods and constraints for reducing this measurement problem to an acceptable level.

SCOPE AND APPROACH

The configuration of a typical standard reference hydrophone, Fig. 1, consists of a pressure sensitive sensor element suspended by a rubber mount inside a metal support frame. This assembly is either immersed in an acoustic coupling liquid, which is contained by a molded rubber boot, or is encapsulated in a thermoplastic elastomer, which has a good acoustic impedance match to that of water. Many standard reference hydrophones have an integral preamplifier whose function is to amplify the sensor output signal and to provide a good match between the high output impedance of the sensor element and the low input impedance of the electrical cable. The sensor element is usually fabricated from the piezoelectric ceramic--lead zirconate-lead titanate.

Three common sensor element configurations used in standard reference hydrophones were analyzed: 1) the radially polarized cylindrical shell, 2) the radially polarized spherical shell, and 3) the axially polarized cylindrical shell. A sensor element when subject to vibration input, produces outputs due to two transduction effects. The first effect is the

Manuscript submitted September 19, 1980.

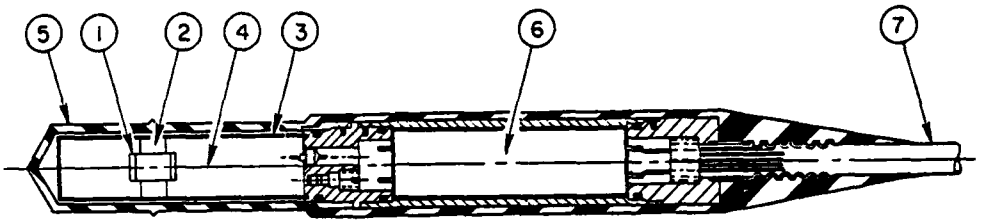

Fig. 1 - Schematic of a typical standard hydrophone.

1 - sensor element
2 - rubber mount
3 - metal support frame
4 - acoustic coupling fluid
5 - molded rubber boot
6 - preamplifier
7 - electrical cable

generation of inertial forces within the piezoelectric material, which produces a voltage output proportional to the acceleration amplitude. The sensor element acts like an accelerometer, which in this case is undesirable. The second effect is that a pressure sensitive sensor when subjected to vertical periodic displacements produces a voltage output proportional to the resultant hydrostatic pressure amplitude. This is because of the high hydrostatic pressure increase with depth in water.

Conclusions from these analyses and experience with the design and use of these sensor configurations are presented to give the designer an opportunity to minimize hydrophone vibration response.

ANALYSES OF RESPONSE TO ACCELERATION

When a piezoelectric hydrophone sensor element is subject to vibration, inertial forces generated within the material of the element produce a voltage output that is proportional to the acceleration amplitude. To determine the voltage output of each sensor configuration due to acceleration, an electromechanical analysis is developed. The following assumptions are made to expedite the analyses and to simplify the final equations:

- Each configuration is a linear system.
- Damping is neglected.
- The cylindrical shell configurations are analyzed assuming a lumped parameter model.
- The acceleration, and therefore displacement, is sinusoidal and in a direction parallel to the axis of symmetry.
- The cylindrical and spherical shells analyzed are thin walled; that is, the inertial stress and forces are constant across any wall cross section.

It will be seen that the assumption of neglecting damping in the analyses of the radially polarized cylindrical and spherical shell configurations will have no effect on the resulting acceleration sensitivity. In the analysis of the axially polarized cylindrical shell.

Radially Polarized Cylindrical Shell

This hydrophone sensor configuration is shown in Fig. 2. It consists, typically, of a radially polarized cylindrical shell made of piezoelectric ceramic. The interior of the shell contains air and is acoustically shielded by rigid end caps hermetically sealed at each end. This assembly is suspended by a rubber mount inside a support frame. The shell has electrodes on its inside and outside surfaces. The rubber mount has three purposes: to provide vibration isolation to the sensor, to accurately position the sensor, and to electrically insulate the outer electrode from the metal support frame.

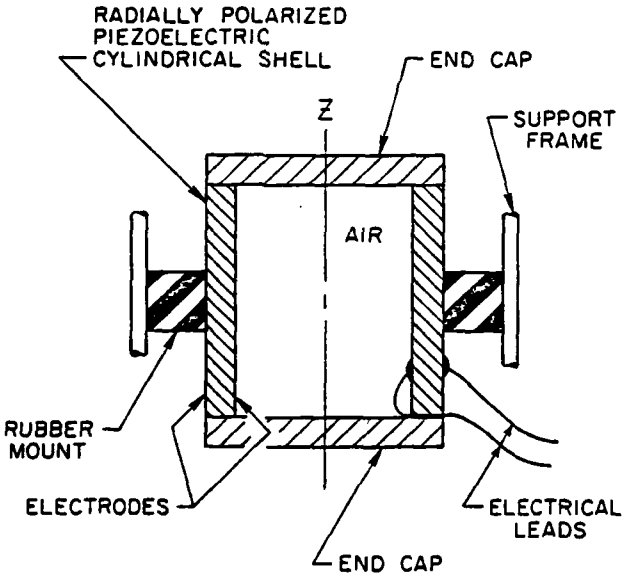

Fig. 2 - Schematic of radially polarized cylindrical shell sensor element. Interior contains air, and exterior is surrounded by acoustic coupling fluid.

A variation in this mounting method was documented by O'Neill[3] in which two piezoelectric cylindrical shells connected in parallel were attached to either side of a support platform.

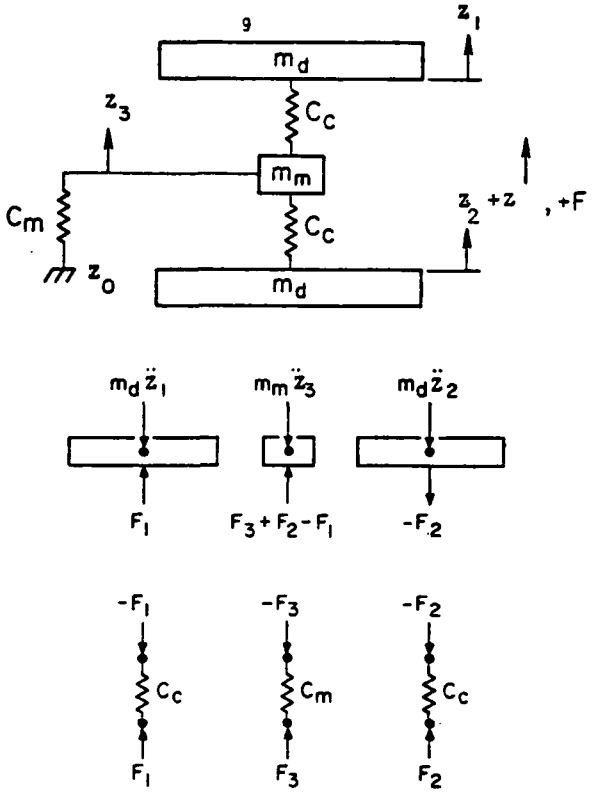

where m_d is combined inertial mass of one end cap and half of cylindrical shell;

m_m is mass of rubber mount;

C_m and C_c are axial mechanical compliances of the mount and half crylindrical shell, respectively;

z_1, z_2, z_3 are displacement amplitudes of the top end cap, bottom end cap, and center of cylindrical shell, respectively;

z_o is the system input displacement of the frame;

F_1, F_2, and F_3 are the force amplitudes on the masses and compliances as shown.

Fig. 3 - Lumped mechanical parameters of radially polarized cylindrical shell sensor element.

Figure 3 shows the lumped mechanical parameter model associated with this sensor configuration. The acceleration response is determined as a function of these parameters, which are under limited designer control.

If F_3 is assumed to be applied uniformly to the wall of the cylindrical shell in a plane perpendicular to the cylindrical axis at its midsection, then $m_d = m_e + m_c/6$. The term $m_c/6$ comes from the equivalent mass of a spring being a third of its total mass, or in this case $(1/3)(m_c/2)$. In this equation, m_e is the mass of an end cap and m_c is the mass of the cylindrical shell. The mass m_m is the lumped mass of the rubber mount and any added inertial mass.

Writing the equations of equilibrium for the inertial forces parallel to the Z axis where z_o is the input displacement amplitude, one has (force and displacement vectors directed up are positive)

$$F_1 - (m_d\ddot{z}_1) = 0, \qquad (1)$$

$$-F_2 - (m_d\ddot{z}_2) = 0, \tag{2}$$

and

$$F_3 + F_2 - F_1 - (m_m\ddot{z}_3) = 0. \tag{3}$$

Equations for the same forces in terms of the compliances are

$$-F_1 + (z_3-z_1)/C_c = 0, \tag{4}$$

$$F_2 + (z_3-z_2)/C_c = 0, \tag{5}$$

and

$$F_3 + (z_3-z_o)/C_m = 0. \tag{6}$$

Solving Eqs. (4), (5), and (6) for the forces, one obtains

$$F_1 = (z_3-z_1)/C_c, \tag{7}$$

$$F_2 = (z_2-z_3)/C_c, \tag{8}$$

and

$$F_3 = (z_o-z_3)/C_m. \tag{9}$$

Let $\omega = 2\pi f$, where f is the frequency in Hz of z_o, and let $\ddot{z}_1 = -\omega^2 z_1$, $\ddot{z}_2 = -\omega^2 z_2$, and $\ddot{z}_3 = -\omega^2 z_3$. Solving Eqs. (1), (2), (3), (7), (8), and (9) simultaneously gives the equations for the displacement amplitudes

$$z_3 = \frac{z_o}{1-(\omega^2 C_m m_m)+(2C_m/C_c)\left[1-\frac{1}{1-(\omega^2 C_c m_d)}\right]} \tag{10}$$

and

$$z_1 = z_2 = z_3/[1 - (\omega^2 C_c m_d)]. \tag{11}$$

Equations (10) and (11), because of identical masses m_d and compliances C_c, contain only two resonance frequencies even though this model has three degrees of freedom. If $\omega_{r1} = [1/(C_c m_d)]^{\frac{1}{2}}$ and $\omega_{r2} = [1/(C_m m_m)]^{\frac{1}{2}}$, then Eqs. (10) and (11) become

$$z_3 = \frac{z_o}{1-(\omega/\omega_{r2})^2+(2C_m/C_c)\left[1-\frac{1}{1-(\omega/\omega_{r1})^2}\right]} \tag{12}$$

and

$$z_1 = z_2 = z_3/[1-(\omega/\omega_{r1})]^2. \tag{13}$$

The voltage sensitivity of this sensor configuration due to acceleration can then be derived. Forces of amplitudes F_1 and F_2 acting on the cylindrical shell generate a voltage amplitude expressed by $e = (d_{31}/C_E)(F_1+F_2)$, where d_{31} is the piezoelectric charge coefficient and C_E is the electrical capacitance. Substituting Eqs. (7) and (8) into this equation gives the expression

$$e = (d_{31}/C_E C_c)(z_2-z_1). \tag{14}$$

Substituting Eq. (13) into Eq. (14) gives the result

$$e = 0. \tag{15}$$

Radially Polarized Spherical Shell

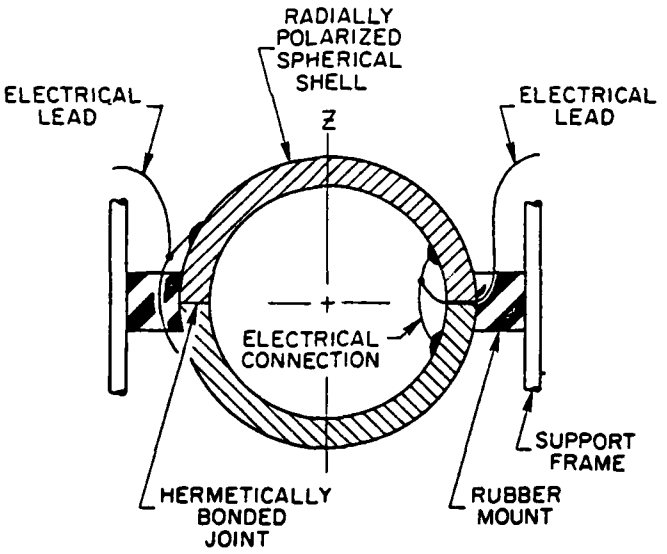

Fig. 4 - Schematic of radially polarized spherical shell sensor element. Interior contains air, and exterior is surrounded by acoustic coupling fluid.

This sensor configuration is shown in Fig. 4, above. It consists, typically, of two thin-walled, radially polarized, piezoelectric hemispheres hermetically bonded together to form a spherical shell. The hemispheres are connected electrically in parallel and have electrodes covering the inside and outside surfaces. The assembly is suspended by a rubber mount inside a support frame, which serves the same purpose as for the cylindrical shell

sensor configuration.

This analysis is based on the theory by Timoshenko [4] with the following additional assumptions:

- A distributed parameter model is assumed.
- There are no shear forces in the shell wall.
- There is no bending of the shell wall.

The equations for the shell bounded by the spherical sector shown in Fig. 5 are

$$2\pi\, a_c N_1(\phi)\, \sin(\phi) + F_z(\phi) = 0 \tag{16}$$

and

$$[N_1(\phi)+N_2(\phi)]/a = -F_s(\phi), \tag{17}$$

where $F_z(\phi)$ is the amplitude in the z direction of all the inertial force acting on the spherical segment of included angle 2ϕ, and $F_s(\phi)$ is the inertial force amplitude per unit area of the same spherical segment in the radial direction, both as a function of ϕ. Deriving the equation for $F_z(\phi)$ from the geometry gives

$$F_z(\phi) = 2\pi\int_o^{\phi} m_s\omega^2 z a a_c d\phi. \tag{18}$$

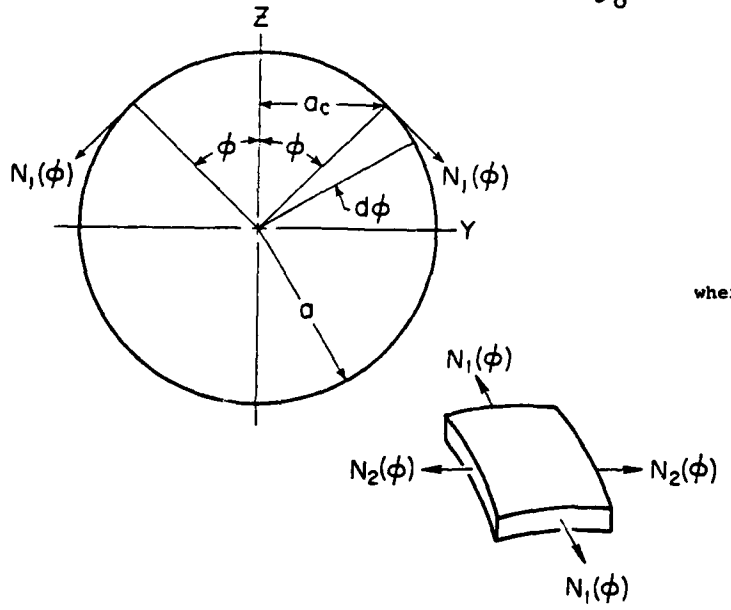

where $N_1(\phi)$ is the tangential component of the inertial force per unit length of shell wall acting on the edge of the spherical segment having included angle 2ϕ and chord mean radius a_c;

$N_2(\phi)$ is the tangential component of the inertial force per unit length of shell wall acting perpendicular to $N_1(\phi)$;

a is the mean radius of the spherical shell.

Fig. 5 - Schematic of inertial forces in the radially polarized spherical shell.

Since

$$a_c = a \sin\phi, \tag{19}$$

m_s is the mass per unit area of the spherical shell, z is the displacement amplitude, and is the same as before, Eq. (18) becomes for the upper hemisphere in Fig. 5, $F_z(\phi) = 2\pi a^2 m_s \omega^2 z \int_0^{\phi} \sin\phi d\phi$. Integrating this expression gives

$$F_z(\phi) = 2\pi a^2 m_s \omega^2 z(1-\cos\phi). \tag{20}$$

Substituting Eqs. (19) and (20) into Eq. (16) gives

$$N_1(\phi) = - \frac{a m_s \omega^2 z}{1+\cos\phi} . \tag{21}$$

Deriving the equation for $F_s(\phi)$ from the geometry of the upper hemisphere yields the result

$$F_s(\phi) = m_s \omega^2 z \cos\phi. \tag{22}$$

Substituting Eqs. (21) and (22) into Eq. (17) gives

$$N_2(\phi) = a m_s \omega^2 z \left(\frac{1}{1+\cos\phi} - \cos\phi\right). \tag{23}$$

If $m_s = \rho_o t$, where ρ_o is the mass density of the piezoelectric ceramic and t is the shell wall thickness, Eqs. (21) and (23) become

$$N_1(\phi) = - \frac{a\rho_o t \omega^2 z}{1+\cos\phi} \tag{24}$$

and

$$N_2(\phi) = a\rho_o t \omega^2 z \left(\frac{1}{1+\cos\phi} - \cos\phi\right). \tag{25}$$

The voltage output amplitude of the upper hemisphere due to acceleration in the z direction as a function of ϕ is then

$$e(\phi) = g_{31}[N_1(\phi) + N_2(\phi)], \tag{26}$$

where g_{31} is the piezoelectric voltage coefficient. Substituting Eqs. (24) and (25) into Eq. (26) gives

$$e(\phi) = - a\rho_o t \, g_{31} \, \omega^2 \, z \cos\phi. \tag{27}$$

The total voltage amplitude generated on the upper hemisphere can be found by integrating Eq. (27), $e_u = - a\rho_o t \, g_{31} \, \omega^2 z \int_0^{\pi/2} \cos\phi d\phi$, or

$$e_u = - a\rho_o t \, g_{31} \, \omega^2 \, z. \tag{28}$$

For the lower hemisphere of Fig. 5, the amplitude of $F_z(\phi)$ will be in the opposite direction to that of the upper hemisphere giving, from Eq. (20), the result

$$F_z(\phi) = - 2\pi a^2 m_s \omega^2 z(1-\cos\phi). \tag{29}$$

Also, the amplitude of $F_s(\phi)$ will be opposite in direction for the lower hemisphere giving from Eq. (22) that

$$F_s(\phi) = - m_s \omega^2 z\cos\phi. \tag{30}$$

Substituting Eqs. (29) and (30) into Eqs. (16) and (17) gives $N_1(\phi) = a\rho_o t\omega^2 z/1+\cos\phi$ and $N_2(\phi) = - a\rho_o t\omega^2 z[(1/1+\cos\phi)-\cos\phi]$. Substituting these equations into Eq. (26) and integrating to find the voltage output amplitude of the lower hemisphere, one obtains $e_\ell = a\rho_o t\, g_{31}\omega^2 z$. Since the two hemispheres are connected in parallel and have the same capacitance, the resulting voltage output of the sensor configuration is

$$e_o = \frac{e_u+e_\ell}{2} = 0. \tag{31}$$

Axially Polarized Cylindrical Shell

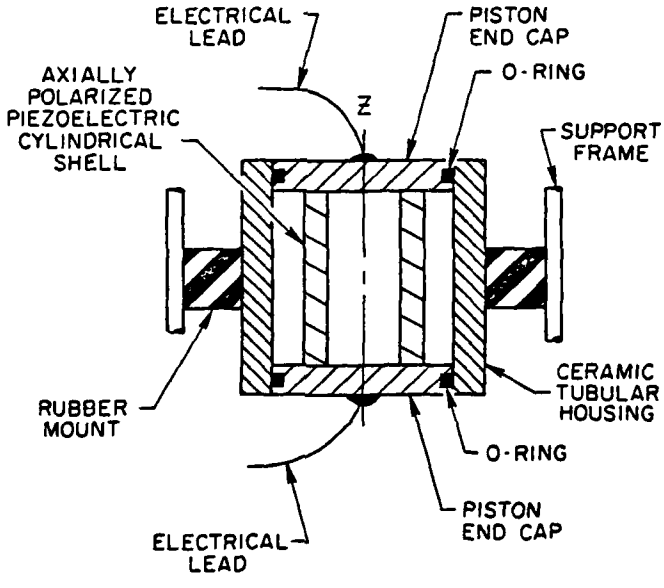

Fig. 6 - Schematic of axially polarized cylindrical shell sensor element. Interior of ceramic tubular housing contains air, and exterior is surrounded by acoustic coupling liquid.

The hydrophone sensor configuration is shown in Fig. 6. It consists of an axially polarized piezoelectric cylindrical shell with a piston end cap cemented to each end. This assembly is sealed concentrically by O-rings inside an air-filled tubular housing made of aluminum oxide material. The O-rings provide a high compliance suspension to the inner assembly and seal it inside the housing. The dielectric housing electrically insulates the piston end caps that act as electrodes for the piezoelectric tube. Also, the housing acoustically shields the inner assembly so that only the outside faces of the piston end caps are exposed to sound pressure. The sensor element is suspended by a rubber mount inside a support frame at its midpoint.

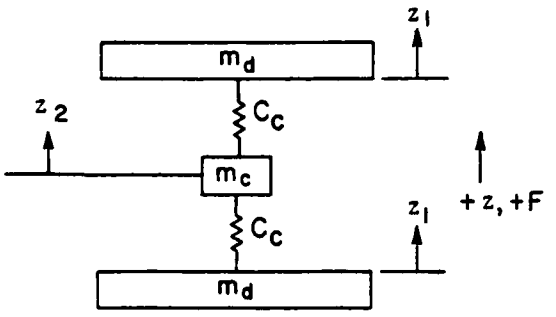

where m_d is the inertial mass of one end cap;

m_c is the inertial mass of the cylindrical shell;

C_c is the axial mechanical compliance of half of the cylindrical shell;

z_1 is the displacement amplitude of both end caps;

z_2 is the displacement amplitude of the inertial mass of the cylindrical shell.

Fig. 7 - Lumped mechanical parameters of axially polarized cylindrical shell sensor element.

Figure 7 shows the lumped mechanical model associated with this sensor configuration. This analysis assumes that the piezoelectric cylindrical shell has a dynamic mass m_c whose displacement is z_2 and having total compliance $2C_c$. The acceleration response derived is for vertical displacement amplitude z_1, input through the O-rings, to the piston end caps. Because of symmetry, the end-cap displacement is the same amplitude for each.

The voltage amplitude out of the sensor element due to these displacements is, by a derivation, similar to that for Eq. (14):

$$e = (d_{33}/C_E C_c)(z_1 - z_2 + z_2 - z_1) = 0, \qquad (32)$$

where d_{33} is the piezoelectric charge coefficient and the other parameters (C_E and C_c) are the same as given for Eq. (14).

ANALYSIS OF RESPONSE TO VERTICAL DISPLACEMENTS

A pressure sensitive hydrophone sensor element when subject to vertical vibration in water produces a voltage output because of the resultant periodic hydrostatic pressure change. This is because in water there is a pressure increase, with depth, of 10^{10} μPa/m. (This number does not vary more than 4% for fresh or salt water.) A sinusoidal displacement amplitude with

vertical amplitude z will result in an equivalent sound pressure of

$$p = 10^{10} z. \tag{33}$$

This is the sound pressure amplitude that the sensor element will detect even if no sound exists in the water. If the vertical acceleration amplitude component $\ddot{z}$ is known, then

$$z = \ddot{z}/\omega^2; \tag{34}$$

and substituting this into Eq. (33) gives an equivalent sound pressure of

$$p = 10^{10} \ddot{z}/\omega^2. \tag{35}$$

If the free field voltage sensitivity of the hydrophone sensor element is

$$(M_e)_h = e/p, \tag{36}$$

where e is the open circuir voltage output for sound pressure p, then the voltage sensitivity to a vertical displacement amplitude z is

$$(M_e)_d = (e/p)(p/z) = e/z. \tag{37}$$

Substituting Eqs. (33) and (36) into this equation results in

$$(M_e)_d = 10^{10} (M_e)_h. \tag{38}$$

These equations can be used to calculate the maximum allowable pressure amplitude because of vertical displacement of a hydrophone for accurate acoustic measurements. Assume the output of the hydrophone sensor element is the sum of the voltages generated by the sound pressure amplitude and the pressure amplitude due to a vertical displacement in phase and at the same frequency. If this second voltage is considered a noise voltage and a minimum signal-to-noise ratio of 20 dB (20 log 10) is desired, then from Eqs. (36) and (37), $(M_e)_h p/(M_e)_d z_a \geq 10$, where z_a is the maximum allowable vertical displacement amplitude. Substituting Eq. (38) into this equation gives

$$z_a \leq 10^{-11} p. \tag{39}$$

To express this equation in more common units, solve for p in the equation

$$SPL = 20 \log(p/p_o), \tag{40}$$

where SPL is the sound pressure level in dB and p_o is a reference sound pressure of 1 μPa. This gives, by substituting the expression for p from Eq. (40) into Eq. (39), the result

$$z_a \leq 10^{(SPL/20)-11}. \tag{41}$$

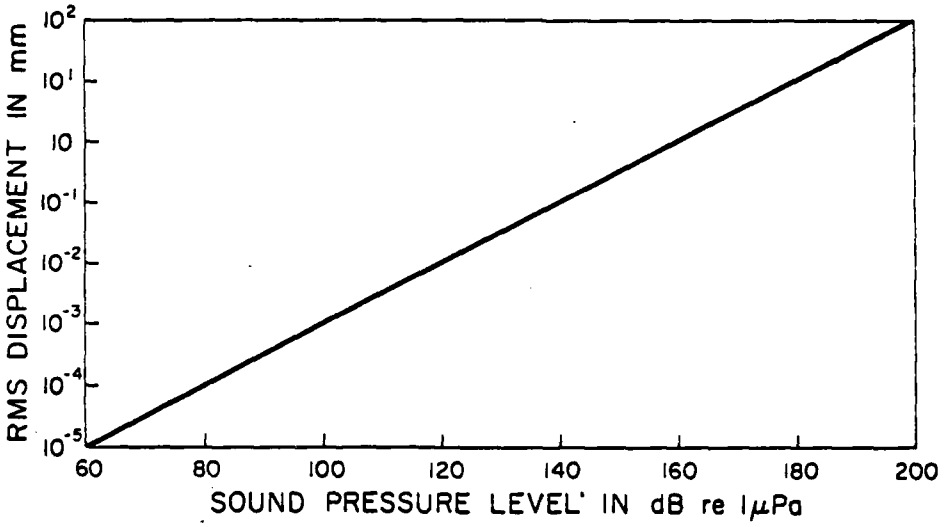

Fig. 8 - Plot of Eq. (41) showing maximum hydrophone displacement amplitude vs. SPL to achieve 20-dB signal-to-noise ratio when signal and noise frequencies are coincident and in phase.

Figure 8 is a plot of Eq. (41). It shows, for a 20-dB signal-to-noise ratio, the maximum allowable rms displacement versus a typical range of SPL's measured in the ocean when the signal and noise frequencies are coincident and in phase.

If the maximum permissible vertical acceleration amplitude is desired, substituting Eq. (34) into Eq. (41) gives

$$\ddot{z}_a \leq \omega^2 10^{(SPL/20)-11}. \tag{42}$$

Therefore, by multiplying the displacement values obtained from Eq. (41) or Fig. 8 by ω^2, the maximum allowable vertical acceleration amplitude can be calculated as a function of frequency.

Hydrophones used for ambient noise measurements at sea are often subject to large vertical displacements due to surface wave conditions that predominate in a continuous spectrum of .03 to 1.0 Hz. Acoustic measurements in this frequency range include typical SPL's as low as 121 dB re 1 μPa at 1 Hz [5], which from Eq. (41) results in a .011-mm, rms maximum allowable displacement amplitude. This displacement amplitude would be exceeded by a hydrophone suspended from floating structures where surface wave heights of 0.3 m or larger result from the predominant sea states of number 2 or greater. These displacement inputs could conceivably be isolated from a hydrophone by employing a mechanical isolation mount. The critical parameter of the mount would be its mechanical compliance, which can be calculated from

$$f_o = (1/2\pi)(1/C_m m_h)^{1/2}, \quad (43)$$

where f_o is mount natural frequency, C_m is the mount compliance, and m_h is the hydrophone mass. From reference [6], the required natural frequency f_o to achieve a 90% reduction in displacement with a damping ratio of 0.5 would be one tenth of the lowest operating frequency. In this case, the lowest operating frequency is .03 Hz; thus f_o would be .003 Hz. For a typical value of m_h of 2 kg, Eq. (43) gives a mount compliance of 1410 m/N (2.47×10^5 in./lbf).

Excessive sensor voltage outputs caused by periodic vertical displacements in the .03 to 1.0-Hz frequency range can prevent acoustic measurements above 1 Hz by causing electrical blockage of the hydrophone preamplifier. Substituting Eq. (33) into Eq. (36) and solving for z gives

$$z_b = 10^{-10} e_b/(M_e)_h. \quad (44)$$

Here the parameters are z_b, the maximum allowable rms hydrophone displacement amplitude; e_b, the sensor output voltage causing the onset of electrical blockage; and $(M_e)_h$, as defined before. Values of these parameters for a typical noise-measuring hydrophone are $(M_e)_h$ = -183 dB re 1 V/μPa and e_b = 0.5 V, giving z_b = 71 mm rms.

CONCLUSIONS AND RECOMMENDATIONS

The radially polarized cylindrical shell, the radially polarized spherical shell, and the axially polarized cylindrical shell sensor configurations have zero voltage sensitivity to acceleration inputs on the axis of symmetry analyzed at any frequency, as shown by Eqs. (15), (31), and (32). Little damping is inherent in the piezoelectric ceramic sensor material and has been realistically neglected in the analysis. The rubber sensor mount and acoustic coupling fluid provide high damping, but neglecting this does not affect the acceleration sensitivity analyzed because of the voltage cancellation effect inherent in these configurations. These sensor configurations are sensitive to acceleration inputs in directions other than that analyzed. Therefore, hydrophone designs employing these sensor types should be oriented so that vibration inputs are confined to the axis of zero acceleration sensitivity. This can be achieved by the orientation of the sensor element within the hydrophone and the hydrophone mounting orientation in the system.

Consideration of the analysis of hydrophone response to periodic vertical displacements results in several conclusions. Equation (41) shows that the maximum vertical displacement amplitude that can be permitted to achieve at least a 20-dB signal-to-noise ratio is independent of frequency and hydrophone acoustic sensitivity. The impossibility of achieving the required displacement isolation over the frequency range of .03 to 1.0 Hz that occurs in acoustic measurements at sea is pointed out by the extremely high isolation mount compliance calculated from Eq. (43) in the analysis. A mount having a compliance of 1410 m/N would be impossible to construct. Therefore, a hydrophone must be removed from the effect of surface wave motion in order to make accurate acoustic measurements due to the extreme sensitivity to vertical displacements shown in Fig. 8. However, displacement isolation

can be achieved at higher frequencies by a properly designed mechanical isolation mount. This can be seen by examination of Eq. (43), which shows that the required isolation mount compliance is inversely proportional to the square of its resonance frequency.

The effect of an excessive sensor voltage output causing electrical blockage of the hydrophone preamplifier can be predicted by inspection of Eq. (44). The maximum displacement amplitude is proportional to the blocking voltage and inversely proportional to the hydrophone sensor acoustic sensitivity. The small magnitude of z_b calculated for a typical noise measuring hydrophone in the analysis points out the severe constraint placed on this parameter. Protection against excess sensor voltage can be provided by diode protection of the preamplifier input [7]. Protection can also be achieved by designing the preamplifier gain characteristics to give a -3 dB break frequency that is as far as possible above the frequency where the excess sensor voltage output occurs. Attenuation of this voltage is achieved as frequency decreases at the rate of -6 dB per octave below the break frequency.

It is recommended that the problem of hydrophone vibration sensitivity be minimized by the following design considerations. First an analysis of the system in which the hydrophone is to be used should be made. The critical parameters to be determined are the hydrophone displacement or acceleration input amplitudes and their corresponding frequencies, the latter of which is more easy to predict.

If the vibration input frequencies are within the acoustic measurement frequency range, then, if possible, one should determine if vibration amplitudes exist that could compromise acoustic measurement accuracy. This can be predicted by the use of Eq. (41) and vibration testing under simulated conditions. It must be kept in mind that vibration-induced noise voltage is the sum of the voltage caused by acceleration added to that caused by vertical displacement. The vibration sensitivity of the hydrophone can then be reduced by two methods. First the hydrophone should be configured so that the predominant vibration inputs are confined to the sensor axis having the smallest acceleration sensitivity. Second, one should provide for the mechanical isolation of the hydrophone from vibration inputs if the excitation frequencies are high enough that a practical isolation mount can be constructed (Eq. 43). If the vibration input frequencies are not within the acoustic measurement frequency range but will cause excessive hydrophone sensor voltage outputs (Eq. 44), then one method of dealing with the problem is attenuation of the sensor output by appropriate preamplifier design.

In summary, vibration is an environmentally induced noise problem that must be considered in the design of standard reference hydrophones used to make measurements in the ocean. The acceleration amplitude to which any sensor configuration is exposed is proportional to the frequency of vibration squared, while sensitivity to vertical displacement amplitude is independent of frequency. Also, hydrophones used in the ocean are usually subjected to large vertical displacements at frequencies in the infrasonic and low audio range. Therefore, noise outputs due to vibration inputs to a hydrophone are dominated by the effect of vertical displacement sensitivity at low frequencies and acceleration sensitivity at higher frequencies.

ACKNOWLEDGMENT

This work was supported by the Naval Research Laboratory under S02-31.701, subproblem /204. Mr. Hugus wishes to thank the Underwater Sound Reference Detachment for the financial and technical support necessary for the production of this report, which was originally written as his masters degree thesis. Also, the author wishes to individually thank D. A. Beard and L. R. Jevnager for their typing services, and Dr. Richard C. Rapson, Jr., as Florida Technological University Faculty Advisor.

REFERENCES

1 - T.A. Henriquez, "An extended-range hydrophone for measuring ocean noise," J. Acoust. Soc. Am. 52, Nov 1972, pp 1450-55.

2 - I.D. Groves, "A Hydrophone for Measuring Acoustic Ambient Noise in the Ocean at Low Frequencies (USRD Type H62)," NRL Report 7738, Apr 1974,

3 - E.T. O'Neill, "Hydrophone Development at Hudson Laboratories," Technical Report 108, Hudson Labs of Columbia University, Dobbs Ferry, NY, Sep 1963.

4 - S. Timoshenko and S. Woinowsky-Kreiger, Theory of Plates and Shells, 2nd Ed. (McGraw-Hill Book Co., New York, 1959) pp. 433-37.

5 - G.M. Wenz, "Acoustic ambient noise in the ocean: spectra and sources,", J. Acoust. Soc. of Am. 34 (Dec 1962), pp 1936-56.

6 - C.M. Harris and C.E. Crede, Editors, Shock and Vibration Handbook, 2nd Ed. (McGraw-Hill Book Co., New York, 1976) pp 2-12 & 2-13.

7 - C.K. Brown and A.C. Tims, "Hydrophone Preamplifier Optimization--Hybrid Microelectronics for Low-Noise Hydrophones," NRL Report 8212, Jun 1978.